

Collective dynamics in sparse networks

Stefano Luccioli,^{1,2,3} Simona Olmi,^{1,2,3} Antonio Politi,^{4,1,3} and Alessandro Torcini^{1,2,3}

¹*CNR - Consiglio Nazionale delle Ricerche - Istituto dei Sistemi Complessi,
via Madonna del Piano 10, I-50019 Sesto Fiorentino, Italy*

²*INFN Sez. Firenze, via Sansone, 1 - I-50019 Sesto Fiorentino, Italy*

³*Centro Interdipartimentale per lo Studio delle Dinamiche Complesse,
via Sansone, 1 - I-50019 Sesto Fiorentino, Italy*

⁴*Institute for Complex Systems and Mathematical Biology and SUPA,
University of Aberdeen, Aberdeen AB24 3UE, United Kingdom*

(Dated: August 6, 2012)

The microscopic and macroscopic dynamics of random networks is investigated in the strong-dilution limit (i.e. for sparse networks). By simulating chaotic maps, Stuart-Landau oscillators, and leaky integrate-and-fire neurons, we show that a finite connectivity (of the order of a few tens) is able to sustain a nontrivial collective dynamics even in the thermodynamic limit. Although the network structure implies a non-additive dynamics, the microscopic evolution is extensive (i.e. the number of active degrees of freedom is proportional to the number of network elements).

PACS numbers: 05.45.-a, 05.45.Jn, 87.19.lj, 05.45.Xt

The organization of dynamical phenomena on different scales is a general property of systems out-of-equilibrium, such as those encountered in plasma physics, turbulence, and neuroscience. The simplest instance of this hierarchical organization is the spontaneous emergence of collective behaviour out of a microscopically chaotic dynamics, a phenomenon reminiscent of equilibrium phase-transitions. The first studies of collective dynamics contributed to uncover time-dependent macroscopic states with different degrees of complexity in mean field models [1, 2] and in spatio-temporal chaotic models [3].

Complex networks provide an even more interesting setup for the study of macroscopic phases, since this is the typical structure of many non-equilibrium systems. Most of the studies of network dynamics have been so far devoted to the characterization of synchronized regimes [4, 5], where the single oscillators evolve in a coherent way. However, some preliminary studies, especially of neural networks with stochastic noise [6], have shown that self-sustained macroscopic oscillations can spontaneously arise also when the single elements evolve in a seemingly uncorrelated way. Altogether, the emergence of collective dynamics has been investigated in the presence of various ingredients such as delayed interactions, diversity of the single elements, time-dependent synaptic connections [7–9]. In particular, it is known that disorder may give rise to an extremely rich macroscopic scenario: this is indeed the framework where glassy phenomena have been uncovered [10] and a highly irregular dynamics observed in neural networks [11].

In this Letter, we study several random networks to clarify the role played by the (in-degree) connectivity K (i.e. the number of incoming connections per node) on the onset of collective motion. It is convenient to distinguish between two classes of systems [12]: *massive* networks, where K is proportional to the network size

N ; *sparse* (or strongly diluted) networks, where $K \ll N$, and specifically K is independent of N as $N \rightarrow \infty$. Lattice systems with short-range interactions belong to the latter class. While it is not surprising to observe the onset of a collective motion in massive networks, it is less obvious to predict whether and when this can happen in sparse ones. In a model of leaky integrate-and-fire (LIF) neurons, it has been shown that a finite connectivity can sustain a partially synchronized regime [13]. Here, we show that the emergence of a collective dynamics above a finite critical connectivity K_c is a general and robust property of sparse networks of oscillators. Since K_c turns out to be of the order of a few tens in all models we have investigated, macroscopic motion appears to be rather ubiquitous and possibly relevant in the context of neural dynamics. In our simulations, we have typically assumed that all nodes are characterized by the same connectivity K , but we have verified that the same scenario holds assuming a Poissonian degree distribution with average connectivity K , as in Erdős-Rényi graphs.

Finally, we analyse the microscopic dynamics, irrespective of the presence of the macroscopic phase, finding that it is always extensive (the number of unstable directions, as well as the power contained in the principal components, is proportional to the network size). This property is highly nontrivial, as the network dynamics is non additive (it cannot be approximated with the juxtaposition of almost independent sub-structures, see below). This is at variance with globally coupled systems, which exhibit a non-extensive component in the Lyapunov spectrum [14].

More specifically we study three classes of dynamical systems: (i) units that are chaotic by themselves (logistic maps - LM); (ii) units that may become chaotic as a result of a periodic forcing (Stuart-Landau oscillators - SL); (iii) phase-oscillators that cannot behave chaotically under any forcing (LIF neurons).

Coupled maps. The dynamics on a network of N coupled logistic maps (LM) is defined as

$$x_{n+1}(i) = (1 - g)f(x_n(i)) + gh_n(i) \quad , \quad (1)$$

where $x_n(i)$ represents the state of the i th node ($i = 1, \dots, N$) at time n , the logistic map $f(x) = ax(1 - x)$ rules the internal dynamics, and g is the coupling strength. Finally, $h_n(i) = (1/K) \sum_{j=1}^N S_{ij}f(x_n(j))$ denotes the local field, where S_{ij} is the connectivity matrix: $S_{ij} = 1$ if an incoming link from j to i is present, otherwise $S_{ij} = 0$. It is convenient to introduce the average field \bar{h}_n and its standard deviation σ_h ($\sigma_h^2 = \langle \bar{h}_n^2 \rangle - \langle \bar{h}_n \rangle^2$) [15].

In Fig. 1, σ_h is plotted versus the connectivity K for $a = 3.9$, $g = 0.1$ and increasing network sizes. For low connectivity, σ_h is quite small and decreases as $1/\sqrt{N}$ with the system size (see left inset), i.e. the deviation from zero is a finite-size effect. Above $K_c \simeq 60$, σ_h assumes finite values, independently of the system size, signaling the onset of a collective dynamics. In fact, the right inset in Fig. 1 reveals nontrivial collective oscillations for $K = 500$ and $N = 20,000$ (we have verified that the thickness of the “curve” does not decrease upon increasing the network size - data not shown). The phase-portrait is analogous to that previously obtained in globally coupled maps [2]. This indicates that the evolution of a sparse network reduces, for $K \rightarrow \infty$, to that of its corresponding mean-field version. What is new and a priori non obvious is that a finite and relatively small connectivity suffices to sustain a macroscopic motion.

As for the evolution of the single units, the most appropriate tool to investigate the microscopic dynamics is Lyapunov analysis. In Fig. 2a,b we can see that both below and above K_c the dynamics is characterized by extensive high-dimensional chaos [16, 17], since the spectra of the Lyapunov exponents (LE) $\{\lambda_i\}$ collapse onto one another, when they are plotted versus the intensive variable i/N [18]. In the inset, one can appreciate that the convergence occurs also for the largest LE, at variance with the non-extensive behavior, recently detected in globally coupled networks [14].

In a sparse network, the field $h_n(i)$ fluctuates with i , no matter how large the network is, since $h_n(i)$ is the sum of a finite number of contributions. One way to characterize its variability is by determining the covariance exponents (CE), i.e. the eigenvalues μ_i of the matrix $C_{ij} = \langle \delta h_n(i) \delta h_n(j) \rangle - \langle \delta h_n(i) \rangle \langle \delta h_n(j) \rangle$, where $\delta h_n(i) = h_n(i) - \bar{h}_n$. In 1D spatial systems with periodic boundary conditions such an approach would correspond to determine the spatial Fourier spectrum. In this case, since there is no “wavelength” to refer to, it is natural to order the eigenvalues from the largest to the smallest one. The results for different network sizes are plotted in Fig. 2 versus i/N , (panel c and d refer to K values below and above K_c , respectively). The good data collapse confirms

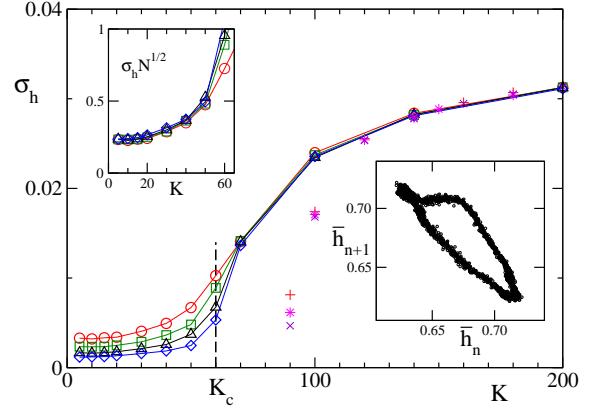


FIG. 1: (color online) Model LM. Standard deviation of the mean field, σ_h (averaged over 5 realizations of disorder) versus K for $N = 5,000$ (red) circles, $N = 10,000$ (green) squares, $N = 20,000$ (black) triangles, and $N = 40,000$ (blue) diamonds. The upper inset shows the rescaled σ_h at low K . In the lower inset the return map of \bar{h}_n for $K = 500$ and $N = 20,000$. Symbols not connected by lines refer to $K = 2N_s + k_R$ ($N_s = 40$ is the number of nearest neighbours and k_R of the random links) for $N = 5,000$ (violet) crosses, $N = 10,000$ (magenta) stars and $N = 20,000$ (red) plus.

the extensivity of microscopic fluctuations. In both panels, μ_i has been rescaled by K , to emphasize extensivity in yet a different way; in fact, as the local field is the sum of K contributions, its variance is expected to be on the order of $1/K$.

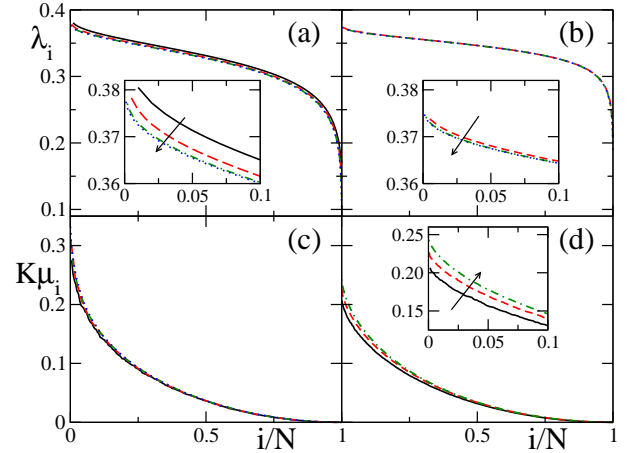


FIG. 2: (color online) Model LM. LE spectra are reported in (a) for $K = 10$ and $N = 100 - 200 - 500 - 1,000$, and in (b) for $K = 80$ and $N = 200 - 500 - 1000$. CE spectra (rescaled by K) are reported in (c) for $K = 10$ and $N = 200 - 400 - 800 - 1,600$, and in (d) for $K = 100$ and $N = 800 - 1,600 - 3,200$. In the insets a zoom of the largest values is shown. In this and in the following figures the arrow direction indicates data obtained for increasing system sizes.

Stuart-Landau oscillators. The second model we have

analysed is a network of Stuart-Landau oscillators (SL),

$$\dot{w}_i = w_i - (1 + ic_2)|w_i|^2 w_i + g(1 + ic_1)(W_i - w_i) \quad , \quad (2)$$

where w_i is a complex variable, and $W_i = (1/K) \sum_{j=1}^N S_{ij} w_j$ represents the local field (S_{ij} is defined as before). Since the local variable is a complex number, it is convenient to introduce the global mean field $W(t) \equiv |\overline{W}|$ (where $|\cdot|$ denotes the modulus operation), which essentially coincides with the Kuramoto order parameter [19]. The data reported for $\langle W \rangle$ in Fig. 3a reveals the discontinuous emergence of some form of synchronization (at least for our choice of the parameter values, $c_1 = -2$, $c_2 = 3$ and $g = 0.47$ [20]). More precisely, there exists a finite parameter range ($55 < K < 85$), where, depending on the initial conditions [22], $\langle W \rangle$ may either vanish or take a finite value. A more precise characterization of the collective phase can be obtained by looking at the variance of the order parameter, namely $\sigma_w^2 = \langle W^2 \rangle - \langle W \rangle^2$. The data in Fig. 3b reveals that the discontinuous transition is accompanied by the birth of temporal fluctuations which increase with the connectivity. As shown in the inset of Fig. 3b, the global attractor exhibits an irregular dynamics. Moreover, it is remarkable that the attractor is qualitatively different from the one found in the mean-field version of the model [21], which is centered around $W \simeq 0.35$.

As for LM, we have verified that both below and above the transition region, the microscopic dynamics is chaotic. In both cases, there is a clear evidence of a convergence towards an asymptotic LE spectrum (the LE spectra for $K = 10$ are reported in Fig. 3c). Analogous conclusions can be drawn from the CE spectra (see Fig. 3d).

Leaky integrate and fire neurons. Finally, we have considered LIF pulse-coupled neurons. They are among the most popular and yet simple models used in computational neuroscience, the field where understanding the onset of collective motion is likely to have the deepest impact. The evolution equation for the membrane potential v_i , writes as $\dot{v}_i = a - v_i + ge_i$, where the local field e_i satisfies the equation [23]

$$\ddot{e}_i + 2\alpha\dot{e}_i + \alpha^2 e_i = \frac{\alpha^2}{K} \sum_{n|t_n < t} S_{il(n)} \delta(t - t_n) \quad . \quad (3)$$

Whenever the membrane potential v_l reaches the threshold $v_l = 1$, it is instantaneously reset to the value $v_l = 0$ and a so-called α -pulse is emitted towards the connected neurons (for more details see [23]). In this case, we introduce the mean field $E = \overline{e}_i$ and the corresponding standard deviation σ_E . The model has been simulated for $a = 1.3$, excitatory synaptic strength $g = 0.2$ and inverse pulse-width $\alpha = 9$. For such values, it is known that in the global coupling limit, there exists a periodic collective motion accompanied by a quasi-periodic microscopic dynamics [24]. For small K , the mean field

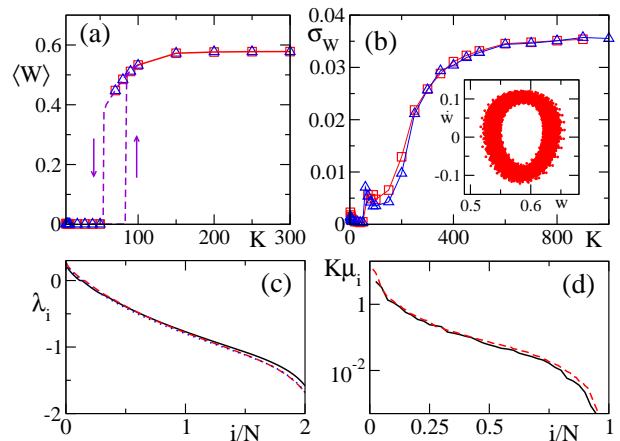


FIG. 3: (color online) Model SL. Average (a) and standard deviation (b) of W versus K for $N = 10,000$ (red) squares, and $N = 20,000$ (blue) triangles (averaged over 5 realizations of the disorder). The dashed lines in (a) show the region of bistability (see the text). The inset in (b) shows the macroscopic attractor for $N = 10,000$ and $K = 800$. (c) LE spectra for $K = 10$ and $N = 100-200-400$. (d) CE spectra (rescaled by K) for $K = 10$ and $N = 40-80$.

is constant in the thermodynamic limit, revealing a so-called asynchronous state, while above a critical value $K_c \approx 9$, it oscillates periodically, as seen in the inset of Fig. 4a. As in the previous systems, the Lyapunov analysis reveals an extensive behaviour, including the initial part (see the two insets), where at finite-size corrections of order $1/N$ are detected. This is to be contrasted with the initial non extensive “layer” observed in globally coupled systems [14]. Fully extensive behaviour was already observed for the Θ -neuron model in [25]. Finally, extensivity is confirmed by the orthogonal decomposition applied to the fluctuations of the local field e_i (see the CE spectra shown in Fig. 4c).

Discussion. By studying three different models, we find that a finite connectivity is able to sustain a non-trivial collective motion, as signalled by the appearance of finite temporal fluctuations of the mean field. This scenario emerges in LMs, whose entire Lyapunov spectrum is positive, as well as in LIF neurons that cannot behave chaotically as stand-alone devices, even when subject to an irregular forcing. The differences among the various models concern the nature of the transition (continuous in LMs and LIF neurons, discontinuous and hysteretic in the SL oscillators) and the complexity of the collective phase that is periodic in LIF neurons but certainly higher dimensional in the other two models. It is desirable to trace back analogies and differences to some general properties of the single systems. In this perspective, it is natural to assume that a finite connectivity acts as a mean field accompanied by an effective noise (due to the “statistical” differences among the fields seen by the

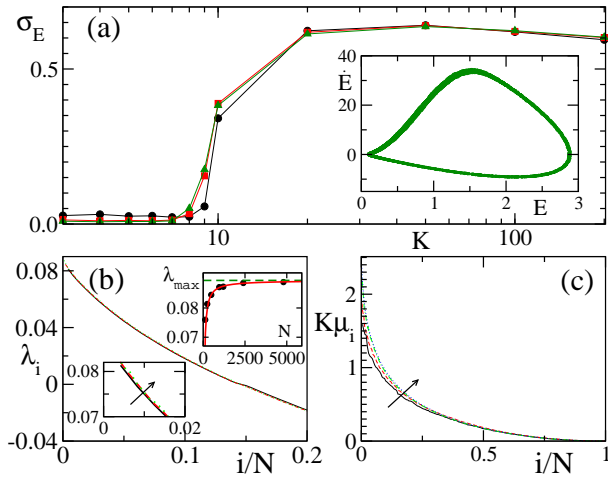


FIG. 4: (color online) Model LIF. (a) Standard deviation of the mean field, σ_E , versus K for $N = 1,000$ (black) circles, $N = 5,000$ (red) squares, $N = 10,000$ (green) triangles. The inset shows the macroscopic attractor for $N = 5,000$ and $K = 200$. (b) LE spectra (in the lower inset a zoom of the largest values) for $K = 20$ and $N = 240–480–960$. In the upper inset the maximum Lyapunov exponent, λ_{max} , versus N is shown, the (red) line represents the nonlinear fit $\lambda_{max} = 0.0894 - 2.3562/N$ and the (green) dashed line marks the asymptotic value. (c) CE spectra (rescaled by K) for $K = 20$ and $N = 200 – 400 – 800 – 1600$.

different nodes). Accordingly, one expects that a small K corresponds to a large noise and is thereby unable to maintain a global coherence, as indeed observed. This picture is, however, rather qualitative, since the collective motion of SL oscillators markedly differs from that one generated in the mean-field limit, even when $K \approx 800$. Altogether, it is remarkable that a few tens of connections consistently suffice to sustain a collective motion in such different environments.

In order to shed further light on the phenomenon, we have added a spatial structure, by organizing the nodes along a line and adding finite-distance interactions. When only the latter are present, no collective motion can arise, because of the low dimensionality of the lattice [3]. The mixed case corresponds to a “small-world” arrangement [26]; we have imposed that the connectivity is the sum of two contributions ($K = 2N_s + k_R$): a number k_R of random links and $2N_s$ links with the nearest nodes. The data reported in Fig. 1 for $N_s = 40$ shows that it is sufficient to add $k_R = 20$ links to establish a collective dynamics; in other words, in the presence of a lattice structure, a lower number of long-range connections may be necessary, although the overall connectivity is larger. This observation reveals that the network structure plays a nontrivial role in determining the number of links that can sustain macroscopic motion.

Next, we comment on the extensive nature of the microscopic motion, a property that is much less obvious

than one could think. In fact, the existence of a limit Lyapunov spectrum in regular lattices is the natural consequence of the additivity of the dynamics [16]. Imagine to use a hyperplane \mathbf{P} to divide a spatial domain of size N into two subdomains \mathbf{S}_1 and \mathbf{S}_2 of size $N/2$. The mutual interaction between \mathbf{S}_1 and \mathbf{S}_2 is negligible as it affects only the interfacial region around \mathbf{P} (it is a “surface” effect). As a result, the entire system can be approximately seen as the juxtaposition of two independent subsets. In the case of sparse networks, it is not even obvious how to split them in two minimally-connected components $\mathbf{S}_1, \mathbf{S}_2$. This problem goes under the name of graph bipartitioning; it is known to be NP complete, and, more important, the solution involves a number of connections that is proportional to N itself, whenever $K > 2 \log 2$ [27, 28]. Therefore, the “interface” cannot be likened to a “surface” and the evolution is necessarily non-additive. Accordingly, the extensive nature of the microscopic evolution is due to subtle properties, that have yet to be clarified.

Conclusions and open problems. In this Letter we have shown that a double-scale (microscopic/macrosopic) evolution is a generic feature of sparse networks. Altogether, the existence of a critical connectivity separating asynchronous from coherent activity is similar to what experimentally observed in neuronal cultures [29]. In the perspective of understanding the conditions for the onset of this behavior, it will be worth exploring the dependence on the coupling strength. In particular, in the weak coupling limit, it might be possible to develop an analytic treatment (as already done for the synchronization transition in LIF neurons [13]), although some of the temporal complexity might be lost.

AT acknowledges the VELUX Visiting Professor Programme 2011/12 for the support received during his stay at the University of Aarhus (Denmark).

-
- [1] K. Kaneko, Phys. Rev. Lett. **65**, 1391 (1990).
 - [2] T. Shibata, T. Chawanya, and K. Kaneko, Phys. Rev. Lett. **82**, 4424 (1999).
 - [3] H. Chaté and P. Manneville, Europhys. Lett. **14**, 409 (1991).
 - [4] A. Arenas, A. Díaz-Guilera, J. Kurths, Y. Moreno, C. Zhou, Phys. Rep. **469** (2008) 93.
 - [5] G. Grinstein and R. Linsker, Proc. Nat. Acad. Sci. (USA) **102**, 9948 (2005).
 - [6] N. Brunel and V. Hakim, Neural Comput. **11**, 1621 (1999).
 - [7] M. Timme, F. Wolf, and T. Geisel, Phys. Rev. Lett. **89** (2002) 258701.
 - [8] M. Denker, M. Timme, M. Diesmann, F. Wolf, and T. Geisel Phys. Rev. Lett. **92** (2004) 074103.
 - [9] Y.L. Maistrenko, B. Lysyansky, C. Hauptmann, O. Burylko, and P. A. Tass, Phys. Rev. E **75** 066207 (2007).
 - [10] M. Mezard, G. Parisi, M. A. Virasoro, *Spin glass theory*

- and beyond* (Singapore, World Scientific, 1987)
- [11] S. Luccioli and A. Politi, Phys. Rev. Lett. **105**, 158104 (2010).
 - [12] D. Golomb, D. Hansel, and G. Mato, in *Handbook of Biological Physics, Vol. 4* p. 887 (Elsevier Science, 2001).
 - [13] D. Golomb, D. Hansel, Neural Comput. **12**, 1095 (2000).
 - [14] K. A. Takeuchi, H. Chaté, F. Ginelli, A. Politi, and A. Torcini, Phys. Rev. Lett. **107**, 124101 (2011).
 - [15] Here and in the following, overlines and angular brackets denote averages over nodes and time, respectively.
 - [16] P. Grassberger, Physica Scripta **40**, 346 (1989).
 - [17] M.R. Paul, M.I. Einarsson, P.F. Fischer, and M.C. Cross, Phys. Rev. E **75**, 045203(R) (2007).
 - [18] R. Livi, A. Politi, and S. Ruffo, J. Phys. A: Math. Gen. **19**, 2033 (1986).
 - [19] Y. Kuramoto, *Chemical Oscillations, Waves, and Turbulence* (Berlin, Springer-Verlag, 1984).
 - [20] Such values have been selected from [21], where the globally coupled version of the model was thoroughly investigated.
 - [21] K.A. Takeuchi, F. Ginelli, and H. Chaté, Phys. Rev. Lett. **103**, 154103 (2009).
 - [22] The hysteresis has been detected by simulating a network where links are first slowly added and then removed.
 - [23] L.F. Abbott and C. van Vreeswijk, Phys. Rev. E **48**, 1483 (1993).
 - [24] C. van Vreeswijk, Phys. Rev. E **54**, 5522 (1996).
 - [25] M. Monteforte and F. Wolf, Phys. Rev. Lett. **105**, 268104 (2010).
 - [26] D. J. Watts and S. H. Strogatz, Nature **393**, 440 (1998).
 - [27] W. Liao, Phys. Rev. Lett. **59**, 1625 (1987).
 - [28] A. G. Percus, G. Istrate, B. Gonçalves, R. Z. Sumi, and S. Boettcher, J. Math. Phys. **49**, 125219 (2008).
 - [29] J. Soriano, M. Rodriguez Martinez, T. Tlusty, and E. Moses, Proc. Natl. Acad. Sci. U.S.A. **105**, 13758 (2008).